Structures of Superdeforemed States in Nuclei with A ∼ 60 Using Two-Parameter Collective Model

N. Gaballah

Physics Department, Faculty of Science (Girls branch), Al-Azhar University, Cairo, Egypt. E-mail: nermgaballah@yahoo.com

Superdeformed (SD) states in nuclei in mass region $A \sim 60-90$ are investigated within the framework of two-parameter formula of Bohr and Motelson model. The concept of γ-ray transition energy E_γ over spin (EGOS) is used to assign the first order estimation of the bandhead spin. The model parameters and the true spin of bandhead have been obtained by adopted best fit method in order to obtain a minimum root-mean-square deviation between the calculated and the experimental γ-ray transition energies. The transition energies E_γ and the dynamical moment of inertia $J^{(2)}$ for data set include thirteen SD bands in even-even nuclei are calculated. The results agree with experimental data well. The behavior of $J^{(2)}$ as a function of rotational frequency $\hbar\omega$ are discussed. By using the calculated bandhead moment of inertia, the predicted quadrupole moments of the studied yrast SD bands are calculated and agree well with the observed data.

1 Introduction

Since the initial discovery of a superdeformed (SD) rotational band in ^{152}Dy [1], several SD bands were identified in different mass region [2]. The SD 60, 80 and 90 regions are of particular interest because they showed exciting new aspects of their large rotational frequency and they present experimental difficulties due to the increased doppler broading of γ-ray peaks and the decreased detection efficiency at large γ-ray transition energies. In $A \sim 60$, the negative-parity SD1 in ^{62}Zn was the first SD band [3], it assigned to configurations with two $ig_{9/2}$ protons (π) and three $ig_{9/2}$ neutrons (ν). It is formed in the $Z = 30$ deformed gap i.e with two $f_{7/2}$ proton holes [4,5]. The SD bands in $A \sim 60$ region are characterized by very large transition energies reaching 3.2 MeV or more. The yrast SD band in Sr was interpreted [6,7] as having the $\nu\, 5^2\pi 5^1$ configuration, i.e the excitation of two $N = 5$, $h_{11/2}$ intruder neutrons, which corresponding to the $N = 44$ shell gap with a large deformation, and a single proton excitation of the $N = 5$, $h_{11/2}$ intruder orbital. The predicted deformation for this band was $\beta_2 \simeq 0.55$ [6]. A systematic analysis on Sr nuclei shows that the quadrupole moment of the SD band in ^{82}Sr is the largest among these Sr isotopes. This may be an indication of the important role of $N = 44$ SD shell gap. For the region $A \sim 90$ SD states with large deformation $\beta_2 \simeq 0.6$ in ^{88}Mo were identified [8]. These findings were in agreement with cranked Woods-Saxon-Strutinsky calculations, which predicted $Z = 42$ and $Z = 43$ to be favored particle numbers at SD shapes in $A \sim 90$ nuclei [8,9].

As it is well known, the experimental data on SD bands consist only in a series of γ-ray transition energies linking levels of unknown spins. Spin assignment is one of the most difficult and unsolved problem in the study of superdeformation.This is due to the difficulty of establishing the deexcitation of a SD band into known yrast states of normal deformed band. Several approaches to assign the spins of SD bands were proposed [10–16]. For all such approaches an extrapolation fitting procedures was used. The purpose of the present paper is to predict the spins of the SD nuclear states in the $A \sim 60-90$ region and to study their properties by using the one-parameter and two-parameters Bohr-Mottelson model. The theoretical formalism is presented in section 2. The theoretical results and a comparison with experimental data are discussed in section 3. Finally a brief conclusion is given in section 4.

2 The formalism

For the strongly deformed nuclei, the collective excitations exhibit a spectrum of rotational character. In even-even nuclei, the spectrum is given by:

$$E(I) = A\,[I(I+1)] \tag{1}$$

where A is the inertial parameter $A = \hbar^2/2J$, with J denoting the effective moment of inertia, which is proportional to the square of the nuclear deformation, and expected to vary slowly with the mass number A. The γ-ray transition energies with the band are given by:

$$\begin{aligned} E_\gamma(I) &= E(I) - E(I-2) \\ &= 4A\left(I - \tfrac{1}{2}\right). \end{aligned} \tag{2}$$

It is interesting to discuss the energy levels by plotting the ratio $E_\gamma(I)$ to spin $(I-\frac{1}{2})$(EGOS)($E-Gamma$ Over Spin) [17] against spin. Therefore, the EGOS for rotational formula (2) can be written as:

$$EGOS = \frac{E_\gamma(I)}{\left(I - \frac{1}{2}\right)} = 4A. \tag{3}$$

Even in a first note on deformed nuclei, Bohr and Mottelson [18] remarked that the simple rotational formula equation (1) gives deviations from experimental data. They pointed out

Table 1: The calculated E Gamma Over Spin (EGOS) for $^{62}Z_n(\mathrm{SD}_1)$ compared to the experimental ones at three bandhead spins $I_0, I_0 \pm 2$ using the one-parameter formula.

$I(\hbar)$	$I_0 = 14.5$ $EGOS\,(\mathrm{keV}/\hbar)$		$I_0 = 16.5$ $EGOS\,(\mathrm{keV}/\hbar)$		$I_0 = 18.5$ $EGOS\,(\mathrm{keV}/\hbar)$	
	exp.	cal.	exp.	cal.	exp.	cal.
16.5	124.562	124.560				
18.5	123.055	124.560	110.722	110.720		
20.5	122.000	124.560	110.750	110.700	99.650	99.648
22.5	122.272	124.560	110.909	110.720	100.681	99.648
24.5	122.458	124.560	112.083	110.720	101.666	99.648
26.5	124.461	124.560	113.038	110.720	103.461	99.648
28.5			115.571	110.720	104.964	99.648
30.5					107.866	99.648

Table 2: The calculated E Gamma Over Spin(EGOS) for $^{62}Z_n(S\,D_1)$ compared to the experimental ones at three bandhead spins $I_0, I_0 \pm 2$ using the two-parameter formula.

$I(\hbar)$	$I_0 = 18$ $EGOS\,(\mathrm{keV}/\hbar)$		$I_0 = 20$ $EGOS\,(\mathrm{keV}/\hbar)$		$I_0 = 22$ $EGOS\,(\mathrm{keV}/\hbar)$	
	exp.	cal.	exp.	cal.	exp.	cal.
20	102.205	101.692				
22	103.023	102.901	92.697	92.477		
24	103.829	104.124	94.255	94.143	84.808	84.607
26	105.490	105.599	95.686	95.957	86.862	86.759
28	106.872	107.304	97.818	97.919	88.727	88.978
30	109.694	109.221	99.627	100.019	91.186	91.280
32			102.730	102.287	93.301	93.678
34					96.597	96.180

that agreement was improved by adding to it a second term (The Bohr-Mottelson two-term formula)

$$E(I) = A[I(I+1)] + B[I(I+1)]^2. \tag{4}$$

The new parameter B is almost negative and is 10^3 times less than that value of A.

$$E_\gamma(I) = A(4I-2) + B\left[2(4I-2)\left(I^2 - I + 1\right)\right], \tag{5}$$

and the EGOS can be written as:

$$\begin{aligned} EGOS &= \frac{E_\gamma(I)}{\left(I - \frac{1}{2}\right)} \\ &= 4A + 8B\left(I^2 - I + 1\right). \end{aligned} \tag{6}$$

For SD bands, one can determine the first-order estimation of the bandhead spin I_0 using equation (2) by calculating the ratio

$$\frac{E_\gamma(I_0+4)}{E_\gamma(I_0+2)} = \frac{E(I_0+4) - E(I_0+2)}{E(I_0+2) - E(I_0)} = \frac{2I_0+7}{2I_0+3}. \tag{7}$$

Let

$$E_{\gamma_1} = E_\gamma(I+2), \tag{8}$$

$$E_{\gamma_2} = E_\gamma(I+4), \tag{9}$$

$$J_0^2 = \frac{4}{E_{\gamma_2} - E_{\gamma_1}}, \tag{10}$$

we can find the bandhead spin I_0 as:

$$I_0 = \frac{1}{2}\left[E_{\gamma_1} J_0^2 - 3\right]. \tag{11}$$

Now, let us define the angular velocity ω as the derivative of the energy E with respect to the spin I

$$\omega = \hbar^{-1}\frac{dE}{d\hat{I}}; \quad \hat{I} = [I(I+1)]^{\frac{1}{2}}. \tag{12}$$

Two possible types of moments of inertia were suggested by Bohr and Mottleson [18] reflecting two different aspects of nuclear dynamics. The kinematic moment of inertia $J^{(1)}$ and the dynamic moment of inertia $J^{(2)}$:

$$J^{(1)} = \frac{\hbar^2}{2}\left[\frac{dE}{d[I(I+1)]}\right]^{-1} = \frac{\hbar}{\omega}[I(I+1)]^{\frac{1}{2}}, \tag{13}$$

Table 3: The bandhead spin proposition and the model parameters A and B adopted from the best fit procedures for the studied SD bands in the $A = 62 - 88$ mass region. The experimental bandhead moment of inertia are also given.

Z	N	Nuclear and the SD band	$E_\gamma(I_0+2\rightarrow I_0)$ (keV)	I_0 ($\hbar$)	A (keV)	B (keV)
30	32	^{62}Zn(SD1)	1993	20	20.997	2.313×10^{-3}
38	42	^{80}Sr(SD1)	1443	16	20.881	-1.873×10^{-4}
		^{80}Sr(SD2)	1688	18	22.106	-1.041×10^{-3}
		^{80}Sr(SD3)	1846	18	24.056	-4.466×10^{-4}
		^{80}Sr(SD4)	2140	20	26.371	-1.705×10^{-3}
38	44	^{82}Sr(SD1)	1429.8	17	19.292	1.770×10^{-4}
40	46	^{86}Zr(SD1)	1518	23	14.732	5.881×10^{-4}
		^{86}Zr(SD2)	1577	16	23.390	-1.354×10^{-3}
		^{86}Zr(SD3)	1866	25	19.082	-1.146×10^{-3}
		^{86}Zr(SD4)	1648	18	22.037	-1.021×10^{-3}
42	46	^{88}Mo(SD1)	1238.6	33	5.788	1.308×10^{-3}
		^{88}Mo(SD2)	1458.6	33	7.676	1.219×10^{-3}
		^{88}Mo(SD3)	1259.1	23	11.406	1.202×10^{-3}

$$J^{(2)} = \hbar^2 \left[\frac{d^2E}{d\left[[I(I+1)]^{\frac{1}{2}}\right]^2} \right] = \hbar \frac{d[I(I+1)]^{\frac{1}{2}}}{d\omega}. \quad (14)$$

$J^{(1)}$ is equal to the inverse of the slope of the curve of energy E versus $\hat{I}^2$ times $(\hbar^2/2)$, while $J^{(2)}$ is related to the curvature in the curve of E versus $\hat{I}$.

In terms of our two-parameter Bohr-Mottleson formula equation (4), yield

$$\hbar\omega(I) = 2\hat{I}\left(A + 2B\hat{I}^2\right), \quad (15)$$

$$J^{(1)}(I) = J_0\left(1 + \frac{2B}{A}\hat{I}^2\right)^{-1}, \quad (16)$$

$$J^{(2)}(I) = J_0\left(1 + \frac{6B}{A}\hat{I}^2\right)^{-1}, \quad (17)$$

with

$$J_0 = \frac{\hbar^2}{2A}. \quad (18)$$

Experimentally the dynamic moment of inertia $J^{(2)}$ is related to the difference ΔE_γ in consecutive transition energies E_γ along a band in the following way

$$\begin{aligned} J^{(2)} &= \frac{dI}{d\omega} \simeq \frac{\Delta I}{\Delta\omega} \simeq \frac{2}{\Delta\left(\frac{E_\gamma}{2}\right)} = \frac{4}{\Delta E_\gamma} \\ &= \frac{4}{E_\gamma(I+2\rightarrow I) - E_\gamma(I\rightarrow I-2)} \end{aligned} \quad (19)$$

remembering that $\omega \simeq E_\gamma/2$. Hence equal ΔE_γ's imply equal $J^{(2)}$'s.

The quadrupole deformation parameter β_2 are derived from the electric quadrupole transition probabilities $B(E_2)$. For this purpose, the well formula [18]

$$B(E_2, I\rightarrow I-2) = \frac{5}{16\pi} Q_0^2 \langle 2020|00\rangle^2, \quad (20)$$

was first applied to extract the intrinsic quadrupole moment Q_0. Then the deformation β_2 of the nuclear charge distribution was derived with the expression [19]

$$Q_0 = \frac{3}{\sqrt{5\pi}} ZR^2\beta_2(1 + 0.36\beta_2) \times 10^{-2}\text{eb} \quad (21)$$

where $R = 1.2\, A^{\frac{1}{3}}$ fm, and Z is the number of protons and A is the number of nucleons.

If X represents the ratio between the major to minor axis of an ellipsoid, then X can be deduced from Q by using the following formula [19]

$$Q = \frac{2}{5} ZR^2 \frac{X^2-1}{X^{\frac{2}{3}}} \times 10^{-2}\text{eb}. \quad (22)$$

The bandhead moment of inertia J_0 is related to the quadrupole deformation β_2 by the Grodzins formula [20]

$$J_0 = c(Z)A^{\frac{5}{3}}\beta_2^2. \quad (23)$$

c(Z) describes the calibration of this relationship between J_0 and β_2.

3 Results and discussions

For each SD band, we used the EGOS concepts of the one-parameter and the two-parameter models equations(3,6) to assign the bandhead spin I_0. Tables (1, 2) and Figure(1) presents

Table 4: Level spin I, γ-ray transition energies E_γ and the dynamical moment of inertia $J^{(2)}$ calculated by using the optimized best parameters listed in Table(3). The experimental γ-ray transition energies are also listed.

^{62}Zn(SD1)				^{80}Sr(SD3)			
E_γ^{exp}(keV)	$I(\hbar)$	E_γ^{cal}(keV)	$J^{(2)}(\hbar^2\text{MeV})^{-1}$	E_γ^{exp}(keV)	$I(\hbar)$	E_γ^{cal}(keV)	$J^{(2)}(\hbar^2\text{MeV})^{-1}$
1993	22	1988.275	17.849	1846	20	1849.857	21.806
2215	24	2212.375	17.054	2039	22	2033.287	22.028
2440	26	2446.915	16.269	2216	24	2214.874	22.275
2690	28	2692.781	15.499	2391	26	2394.445	22.549
2939	30	2950.862	14.750	2572	28	2571.830	22.853
3236	32	3222.048		2747	30	2746.857	
^{82}Sr(SD1)				^{86}Zr(SD1)			
E_γ^{exp}(keV)	$I(\hbar)$	E_γ^{cal}(keV)	$J^{(2)}(\hbar^2\text{MeV})^{-1}$	E_γ^{exp}(keV)	$I(\hbar)$	E_γ^{cal}(keV)	$J^{(2)}(\hbar^2\text{MeV})^{-1}$
1429.8	19	1436.598	25.385	1518	15	1513.088	29.361
1596.6	21	1594.170	25.273	1646	17	1649.323	28.729
1757.7	23	1752.439	25.151	1785	19	1788.551	28.081
1918.6	25	1911.473	25.020	1929	21	1930.996	27.417
2076.6	27	2071.340	24.880	2077	23	2076.886	26.745
2228.6	29	2232.107	24.731	2228	25	2226.446	26.066
2380.7	31	2393.844	24.574	2383	27	2379.901	25.384
2544.6	33	2556.616	24.408	2540	29	2537.478	24.702
2736	35	2720.494		2696	31	2699.403	
^{86}Zr(SD3)				^{86}Zr(SD4)			
E_γ^{exp}(keV)	$I(\hbar)$	E_γ^{cal}(keV)	$J^{(2)}(\hbar^2\text{MeV})^{-1}$	E_γ^{exp}(keV)	$I(\hbar)$	E_γ^{cal}(keV)	$J^{(2)}(\hbar^2\text{MeV})^{-1}$
1866	27	1851.803	36.037	1648	20	1658.218	25.696
1959	29	1962.798	38.197	1811	22	1813.881	26.412
2062	31	2067.518	40.815	1967	24	1965.327	27.241
2155	33	2165.521	44.030	2123	26	2112.163	28.202
2244	35	2256.368	48.048	2273	28	2253.996	29.317
2343	37	2339.618	53.181	2403	30	2390.435	30.615
2429	39	2414.832		2491	32	2521.086	
^{80}Sr(SD4)				^{88}Mo(SD2)			
E_γ^{exp}(keV)	$I(\hbar)$	E_γ^{cal}(keV)	$J^{(2)}(\hbar^2\text{MeV})^{-1}$	E_γ^{exp}(keV)	$I(\hbar)$	E_γ^{cal}(keV)	$J^{(2)}(\hbar^2\text{MeV})^{-1}$
2140	22	2132.134	23.600	1458.6	35	1460.250	29.582
2292.1	24	2301.619	24.723	1595.6	37	1595.465	27.823
2459	26	2463.411	26.068	1740.1	39	1739.226	26.182
2621.1	28	2616.854	27.693	1894.9	41	1892.002	24.652
2763	30	2761.294		2054.2	43	2054.260	23.227
				2224.3	45	2226.469	
^{80}Sr(SD2)				^{88}Mo(SD1)			
E_γ^{exp}(keV)	$I(\hbar)$	E_γ^{cal}(keV)	$J^{(2)}(\hbar^2\text{MeV})^{-1}$	E_γ^{exp}(keV)	$I(\hbar)$	E_γ^{cal}(keV)	$J^{(2)}(\hbar^2\text{MeV})^{-1}$
1688	20	1662.433	25.670	1238.6	35	1228.823	31.877
1821.1	22	1818.252	26.399	1342.1	37	1354.302	29.707
1950	24	1969.772	27.244	1480.7	39	1488.949	27.716
2090	26	2119.593	28.224	1633.5	41	1633.266	25.891
2256	28	2258.315	29.363	1795.5	43	1787.756	24.218
2364.1	30	2394.540	30.692	1962.2	45	1952.921	22.683
2573.9	32	2524.865		2133.4	47	2129.269	21.274
				2306.6	49	2317.284	

Table 6: The calculated quuadrupole deformation parameter β_2 and the major to minor axis ratio X in the yrast SD bands for even-even ^{62}Zn, ^{80,82}Sr, ^{86}Zn and ^{88}Mo nuclei. The experimental quadrupole moments Q^{exp} are also given for comparison.

	J_0 ($\hbar^2$MeV^{-1})	C(Z)	β_2	Q eb	X	Q^{exp} eb
^{62}Zn(SD1)	23.835	0.1261	0.4410	2.6178	1.52	2.70
^{80}Sr(SD1)	24.002	0.1106	0.3822	3.3438	1.44	3.42
^{82}Sr(SD1)	25.917	0.1089	0.3920	3.4973	1.45	3.54
^{86}Zr(SD1)	33.939	0.0996	0.4508	4.4512	1.54	4.60
^{88}Mo(SD1)	86.385	0.1707	0.5390	5.8295	1.66	6.00

Table 5: Level spin I, γ-ray transition energies E_γ and the dynamical moment of inertia $J^{(2)}$ calculated by using the optimized best parameters listed in Table(3). The experimental γ-ray transition energies are also listed.

^{80}Sr(SD1)			
E_γ^{exp}(keV)	$I(\hbar)$	E_γ^{cal}(keV)	$J^{(2)}(\hbar^2\text{MeV})^{-1}$
1443	18	1453.619	24.395
1611	20	1617.584	24.500
1775.1	22	1780.848	24.616
1948	24	1943.338	24.745
2118	26	2104.983	24.886
2284	28	2265.711	25.041
2440.9	30	2425.449	25.208
2595	32	2584.127	25.389
2743	34	2741.672	25.585
2680	36	2898.011	
^{86}Zr(SD3)			
E_γ^{exp}(keV)	$I(\hbar)$	E_γ^{cal}(keV)	$J^{(2)}(\hbar^2\text{MeV})^{-1}$
1577	18	1579.123	24.266
1730	20	1743.961	25.036
1890	22	1903.730	25.944
2056	24	2057.908	27.014
2227	26	2205.976	28.280
2392	28	2347.414	29.786
2514	30	2481.702	31.591
2562	32	2608.320	33.776
2708	34	2726.748	
^{88}Mo(SD3)			
E_γ^{exp}(keV)	$I(\hbar)$	E_γ^{cal}(keV)	$J^{(2)}(\hbar^2\text{MeV})^{-1}$
1259.1	25	1259.498	31.051
1382.6	27	1388.315	29.644
1522.9	29	1523.249	28.265
1669.4	31	1664.763	26.926
1817.0	33	1813.317	25.631
1976.0	35	1969.375	24.386
2134.0	37	2133.397	23.195
2297.0	39	2305.846	

the numerical values and graph of EGOS at three different values of bandhead spins I_0, $I_0 \pm 2$ for the yrast SD band in ^{62}Zn as example for our calculations. The model parameters

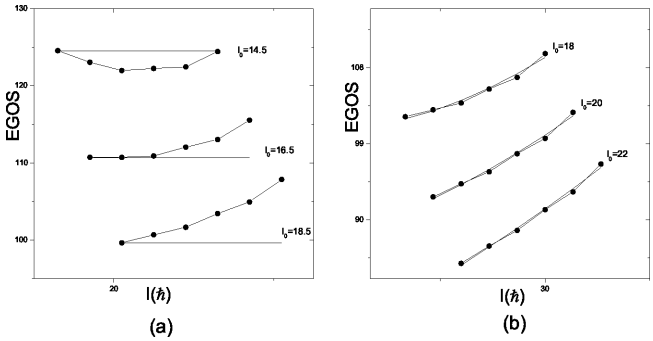

Fig. 1: Calculated (solid lines) and experimental (closed circles) EGOS against spin I for these different values of bandhead spin $I_0, I_0 \pm 2$. (a) for first order estimation of I_0 (b) for second order estimation of I_0.

A and B are then fitted to reproduce the observed transition energies E_γ. The procedure is repeated for several trail values of A and B and recalculate the true spin of the lowest observed level. In order to illustrate the sensitivity of the root mean square deviation, we employed the common definition of the chi squared

$$\chi^2 = \frac{1}{N}\sum_i \left[\frac{E_\gamma^{exp}(I_i) - E_\gamma^{cal}(I_i)}{\Delta E_\gamma^{exp}(I_i)}\right]^2 \qquad (24)$$

where N is the number of data points and ΔE_γ^{exp} is the experimental error in γ-ray transition energies. The experimental data are taken from the evaluated nuclear structure data file ENSDF [2]. Table (3) lists the bandhead spin proposition and the adopted model parameters. Using the best fitted parameters, the spins I, the γ-ray transition energies E_γ, the rotational frequency $\hbar\omega$ and the dynamical moment of inertia $J^{(2)}$ are calculated and listed in Table(4) compared to the observed E_γ.

Figures (2, 3, 4) shows the experimental and calculated dynamical moment of inertia $J^{(2)}$ as a function of rotational frequency $\hbar\omega$ for the SD bands in our even-even nuclei. The experimental and calculated values are denoted by solid circles and solid lines respectively.

By substituting the calculated bandhead moment of inertia J_0 in Grodzins formula equation (23), we adjusted the pro-

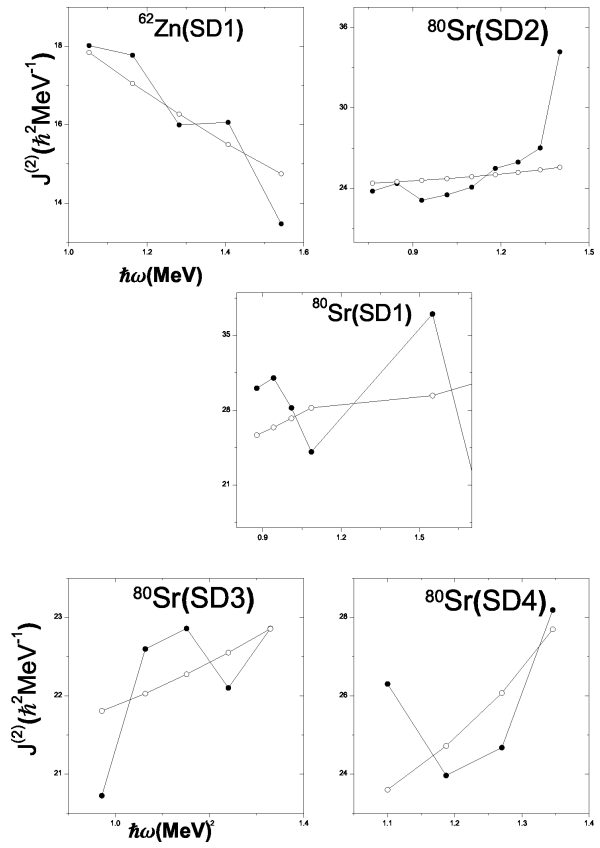

Fig. 2: Shows the experimental and calculated dynamical moment of inertia $J^{(2)}$ as a function of rotational frequency $\hbar\omega$ for even-even ^{62}Zn(SD1) and ^{80}Sr(SD1, SD2, SD3 and SD4). The experimental and calculated values are denoted by solid circles and solid lines respectively.

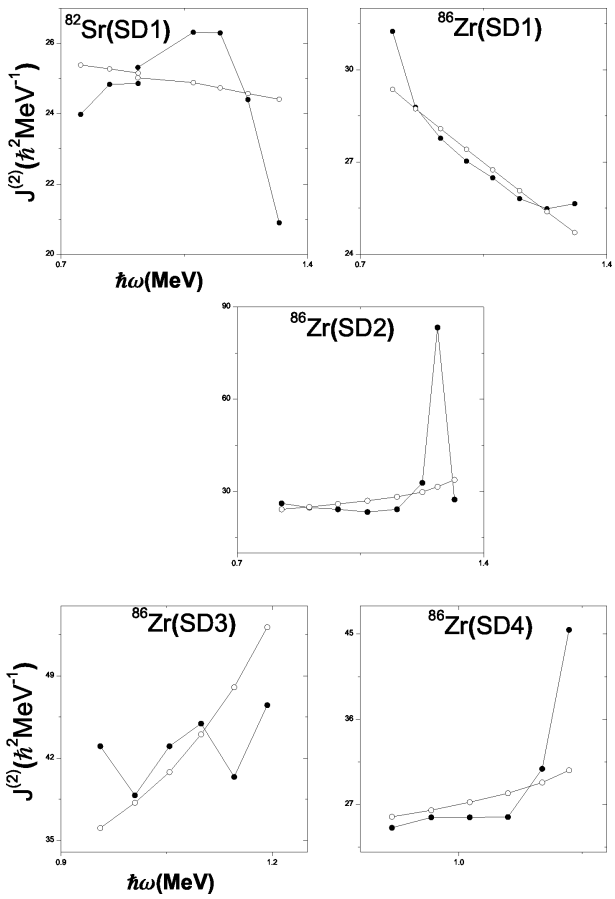

Fig. 3: Shows the experimental and calculated dynamical moment of inertia $J^{(2)}$ as a function of rotational frequency $\hbar\omega$ for even-even ^{82}Sr(SD1) and ^{86}Zn(SD1, SD2, SD3 and SD4). The experimental and calculated values are denoted by solid circles and solid lines respectively.

portional constant c(Z) for each yrast SD band and extracted the deformation parameter β_2 and then calculated the transition quadrupole moment Q which is related to the ratio X of the major to minor axis. The results are given in Table (5).

4 Conclusion

The structure of the SD bands in the mass region $A \sim 60-90$ have been investigated in the framework of two-parameter Bohr-Mottelson model. The bandhead spins have been extracted by using first order estimation method using the concept of EGOS. The model parameters have been determined by using a best fit method between the calculated and the experimental transition energies. The calculated transition energies E_γ, rotational frequency $\hbar\omega$ and dynamic moments of inertia $J^{(2)}$ are all well agreement with the experimental ones. This confirm that our model is a particular tool in studying the SD rotational bands. The behavior of $J^{(2)}$ as a function of $\hbar\omega$ have been discussed. The quadrupole deformation parameters are also calculated.

Submitted on December 5, 2014 / Accepted on December 12, 2014

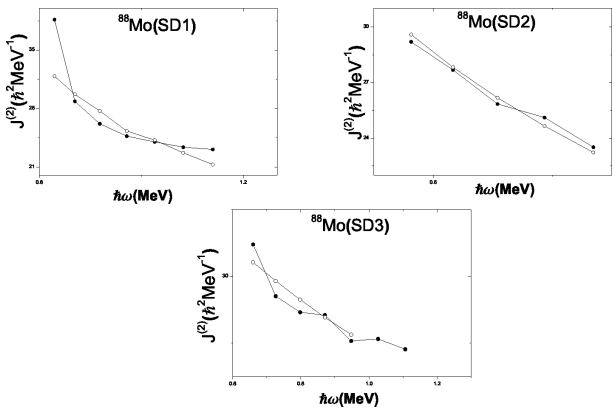

Fig. 4: Shows the experimental and calculated dynamical moment of inertia $J^{(2)}$ as a function of rotational frequency $\hbar\omega$ for even-even ^{88}Mo(SD1, SD2 and SD3). The experimental and calculated values are denoted by solid circles and solid lines respectively.

References

1. Twin P. J. , Nyak B. M. Observation of a Discrete Line Superdeformed Band up to $60\hbar$ in ^{152}Dy. *Physical Reveiw Letters*, 1986, v. 57, 811–814.
2. National Nuclear Data Center NNDC, Brookhaven National Laboratory, http.//www.nndc.bnl.gov/chart/
3. Svenssan C.E. et al. Observation and Quadrupole-Moment Measurement of the First Superdeformed Band in the $A \sim 60$ Mass Region. *Phys. Rev. Lett.*, 1997, v. 79, 1233.
4. C. H. Yu et al, Comparison of Superdeformation Bands in ^{61}Zn and ^{60}Zn: Possible evidence for $T = 0$ Pairing. *Phys. Rev.* 1999, v. 60C, 031305.
5. Johnasson E.K. et al. *Phys. Rev.*, 2008, v. C77, 064316.
6. Smith A.G. et al. Observation of Superdeformation in ^{82}Sr. *Phys. Lett.*, 1995, v. 355B, 32.
7. Yu C.H. et al. Lifetime Measurements of Normally Deformed and Superdeformed States in ^{82}Sr. *Phys. Rev.*, 1998, v. 57C, 113.
8. Bäck T. et al. Observation of Superdeformed States in ^{88}Mo. *Eur. Phys. J.*, 1999, v. 6A, 391.
9. Cederwall B. et al. Favoured Superdeformed States in ^{89}Tc. *Eur. Phys. J.*, 1999, v. 6A, 251.
10. Becker J.A. et al. Level Spin and Moment of Inertia in Superdeformed Nuclei Near $A = 194$. *Nucl. Phys.*, 1990, v. A520, C187–C194.
11. Droper J.E. et al. Spins in Superdeformed Bands in the Mass 190 region. *Phys. Rev.*, 1990, v. C42, R1791–R1795.
12. Zeng J.Z. et al. Critical of the spin Assignement of Rational Band. *Commun Theor. Phys.*, 1995, v. 24, 425.
13. Goel A. *Int. J. Scientific Research*, 2013, v. 21, 2277.
14. Hegazi A.M., Ghoniem M.H. and Khalaf A.M. Theoretical Spin Assignment for Superdeformed Rotational Bands in Mercury and Lead Nuclei. *Egyptian Journal of Physics*, 1999, v. 30, 293–303.
15. Khalaf A.M. et al. Description of Rotational Bands in Superdeformed Nuclei by Using Two-Parameter Empirical Formula. *Egyptian Journal of Physics*, 2003, v. 34, 159–177.
16. Khalaf A.M., Sirag M.M. and Taha M. Spin Assignement and Behavior of Superdeformed Bands in $A \sim 150$ Mass Region, *Turkish Journal of Physics*, 2013, v. 37, 49–63.
17. Khalaf A. and Okasha M. Properties of Nuclear Superdeformed Rotational Bands in $A \sim 190$ Mass Region. *Progress in Physics*, 2014, v. 10, 246–252.
18. Bohr A. and Mottelson B. Nuclear Structure v.2, Benjamin Inc, New York, 1975.
19. Clark R.M. et al. Very Extended Shapes in the $A \sim 110$ Region. *Phys. Rev. Lett.*, 2001, v. 87, 202502.
20. Grodzins I. *Phys. Lett.*, 1962, v. 2, 88.